An emitted random walk model of gravitational attraction on a cubic lattice

Zoan*

September 9, 2026

Abstract

We formulate a proposed mechanism in which massive bodies emit particles that perform unbiased random walks on a three-dimensional cubic lattice. A registered collision gives a receiving body a momentum impulse opposite the particle's most recent lattice step; particles then continue unchanged. For fixed sources and receivers, we derive the exact mean force from neighboring particle populations. The stationary population is the cubic-lattice Green function. A modified Bessel function identity shows that the point-source mean force is exactly directed toward the source at every nonzero lattice separation, and its magnitude approaches Newton's inverse-square law over many lattice spacings. We express the effective gravitational constant in microscopic parameters and derive a discrete Poisson representation. For many bodies, we prove that voxel population counts and multinomial transfers preserve the synchronous stochastic collision process without storing individual particles or emitter identities. We distinguish this exact aggregation from weighted-particle merging, annihilation, deterministic field evolution, and bounded-state approximations. We also describe fluctuations and diffusion delays and report reproducible numerical checks of the lattice force. The results establish a Newtonian mean-force representation under explicit assumptions. They do not establish microscopic energy or momentum conservation, relativistic propagation, or the physical existence of the particles. The connection between random walks and gravitational potentials is established mathematics; we examine a particular collision interpretation without asserting priority for it.

1 Motivation and scope

The proposed picture is local and discrete. Space is represented by the sites of a cubic lattice. A body emits particles; each emitted particle repeatedly selects one of the six face-adjacent cells; and a collision with another body changes that body's motion. The intended macroscopic effect is attraction between the bodies.

A crucial question is what information a collision uses. A random walk does not retain a straight trajectory from its source, so reversing its most recent step does not generally point to that source on an individual encounter. Nevertheless, the numbers arriving from opposite directions are unequal when the particle population varies in space. A collision rule that reverses each incoming step can convert that imbalance into an average attraction.

*Model proposal by Zoan. Mathematical formalization, numerical calculations, and manuscript preparation developed with assistance from ChatGPT.

We make this rule precise and analyze its stationary mean. We keep the cubic lattice throughout; continuum equations are used only to characterize behavior over many lattice spacings. The core results concern fixed point sources and fixed receivers. A receiver's "force" is its expected accumulated impulse per unit time while held at its specified site. A self-consistent theory of freely moving bodies requires further rules and is not established by the fixed-body calculation.

The connection between random walks, Green functions, and Poisson equations is classical [1]. Random-path methods have already been applied to gravitational potential and acceleration calculations [5], and grid-based gravitational solvers are standard in astrophysical computation [6]. The purpose here is to specify what a particular local collision proposal yields, identify which assumptions produce attraction and mass scaling, and expose the remaining physical requirements. Section 6 addresses a further question: how to simulate many emitters without retaining an ever-growing list of particle objects, and which information a finite voxel representation can safely discard.

2 The microscopic lattice rules

2.1 Space and emitted particles

Fix a lattice spacing $h > 0$. The sites are $h\mathbb{Z}^3$, with integer coordinate $\boldsymbol{n}$ corresponding to physical position $\boldsymbol{x} = h\boldsymbol{n}$. The unit vectors $\boldsymbol{e}_1, \boldsymbol{e}_2, \boldsymbol{e}_3$ label the coordinate directions. There are exactly six allowed displacement vectors, $\pm h\boldsymbol{e}_j$. There are no diagonal hops.

A source of mass $M > 0$, fixed at the origin, emits independent particles according to a Poisson process of rate qM, where $q > 0$ has units of inverse mass per unit time. Each particle subsequently performs a continuous-time random walk with rate $\gamma > 0$ to each particular neighbor. Thus its total hopping rate is 6γ. After an exponentially distributed waiting time of mean $(6\gamma)^{-1}$, it chooses one of the six directions uniformly. The lattice Laplacian in integer coordinates is

$$(\Delta_{\mathbb{Z}} f)(\boldsymbol{n}) = \sum_{j=1}^{3} \big[f(\boldsymbol{n} + \boldsymbol{e}_j) + f(\boldsymbol{n} - \boldsymbol{e}_j) - 2f(\boldsymbol{n})\big]. \tag{1}$$

The generator is $\gamma\Delta_{\mathbb{Z}}$, and the corresponding diffusion coefficient in physical coordinates is $D = \gamma h^2$. Continuous time simplifies the derivation and removes synchronous parity effects. Appendix A gives a version with one hop per clock tick and the same stationary mean force.

2.2 The collision rule

Place a receiver of inertial mass $m > 0$ at a fixed site $h\boldsymbol{n}$. If a particle arrives there by taking the step $h\boldsymbol{s}$, where $\boldsymbol{s} \in \{\pm\boldsymbol{e}_1, \pm\boldsymbol{e}_2, \pm\boldsymbol{e}_3\}$, assign the receiver the impulse

$$\Delta\boldsymbol{P} = -mv_*\boldsymbol{s}, \qquad v_* > 0. \tag{2}$$

Here v_* is a fixed speed scale, so the corresponding velocity increment is $\Delta\boldsymbol{v} = -v_*\boldsymbol{s}$. The particle continues its original random walk, with no change in hopping rates and no removal from the system. Every arrival is registered, including repeated returns by the same particle. Birth at an occupied source site is not itself an arrival event.

This is a nonabsorbing encounter rule. The word collision denotes a local registered interaction; it does not imply the momentum-transfer law of a conventional particle impact. The negative sign in (2) is a postulate. Likewise, choosing an impulse proportional to receiver mass builds mass-independent acceleration into the response law. Neither property is derived from random-walk geometry.

A particle needs its current site and latest step to execute this rule. It need not know the emitter's location or identity. Source labels may be retained for bookkeeping, but they are not required to evaluate a collision.

Parameter	Meaning	Physical units
h	Cubic-lattice spacing	length
q	Emission rate per source mass	mass^{-1} time^{-1}
γ	Hopping rate to each neighbor	time^{-1}
v_*	Velocity change per registered collision	length time^{-1}
$D = \gamma h^2$	Continuum diffusion coefficient	length^2 time^{-1}

3 The particle population and its stationary limit

Let $N(\boldsymbol{n}, t)$ be the random number of particles at site $\boldsymbol{n}$, and let $\mu(\boldsymbol{n}, t) = \mathbb{E}N(\boldsymbol{n}, t)$. Start with no particles at time zero. Write

$$K_t(\boldsymbol{n}) = (e^{t\Delta_{\mathbb{Z}}}\delta_0)(\boldsymbol{n}), \qquad \mathcal{H}(\boldsymbol{n}) = \int_0^\infty K_t(\boldsymbol{n})\, dt. \tag{3}$$

K is the transition kernel when the rate to each neighbor is one. A general rate γ uses $K_{\gamma t}$.

Proposition 3.1 (Mean population)**.** *The mean occupation satisfies*

$$\partial_t \mu = \gamma \Delta_{\mathbb{Z}} \mu + qM\delta_0, \qquad \mu(\boldsymbol{n}, t) = qM \int_0^t K_{\gamma s}(\boldsymbol{n})\, ds. \tag{4}$$

In three dimensions, it increases to a finite value at every fixed site,

$$\mu_\infty(\boldsymbol{n}) = \frac{qM}{\gamma}\mathcal{H}(\boldsymbol{n}), \qquad -\Delta_{\mathbb{Z}}\mathcal{H} = \delta_0. \tag{5}$$

Proof. Every occupied site sends particles to each neighbor at rate γ per particle. Expected inflow minus expected outflow gives the first term in (4); emission gives the source term. Summing the transition probabilities of particles born at all earlier times gives the integral solution. Transience of the simple random walk in three dimensions implies finiteness of the occupation integral. Integrating $\partial_t K_t = \Delta_{\mathbb{Z}} K_t$ from zero to infinity yields $\Delta_{\mathbb{Z}}\mathcal{H} = -\delta_0$, since $K_0 = \delta_0$ and $K_t(\boldsymbol{n}) \to 0$ at each fixed site. □

There is no finite stationary total particle number. Starting empty, the expected number in the entire lattice is qMt. Local stationarity means that walkers diffuse away while a finite mean remains near each specified site. In particular, $\sum_{\boldsymbol{n}} \mu_\infty(\boldsymbol{n}) = \infty$. An infinite lattice, or an explicitly chosen escape boundary, is essential to this distinction.

With the normalization in (3), $\mathcal{H}$ equals one sixth of the usual discrete-time simple-random-walk Green function: the mean holding time is 1/6. Standard estimates give

$$\mathcal{H}(\boldsymbol{n}) = \frac{1}{4\pi|\boldsymbol{n}|} + O(|\boldsymbol{n}|^{-3}), \qquad |\boldsymbol{n}| \to \infty. \tag{6}$$

The corresponding first-difference estimates are also available [1, Theorem 4.3.1 and Corollary 4.3.3]. We use those estimates below rather than differentiating a remainder bound without justification.

4 The exact mean collision force

Let $\boldsymbol{I}(T)$ be the accumulated assigned impulse on the fixed receiver over a time interval of length T. Define $\boldsymbol{F}(\boldsymbol{n},t) = d\mathbb{E}\boldsymbol{I}(t)/dt$. In a stationary particle field this is independent of time.

Proposition 4.1 (Arrival imbalance)**.** *For each coordinate j, the mean force at time t is*

$$F_j(\boldsymbol{n},t) = mv_*\gamma\big[\mu(\boldsymbol{n}+\boldsymbol{e}_j,t) - \mu(\boldsymbol{n}-\boldsymbol{e}_j,t)\big]. \tag{7}$$

Consequently, its stationary value is

$$F_j(\boldsymbol{n}) = mv_*qM\big[\mathcal{H}(\boldsymbol{n}+\boldsymbol{e}_j) - \mathcal{H}(\boldsymbol{n}-\boldsymbol{e}_j)\big]. \tag{8}$$

Proof. Arrivals from $\boldsymbol{n}-\boldsymbol{e}_j$ occur at mean rate $\gamma\mu(\boldsymbol{n}-\boldsymbol{e}_j,t)$. Their last step is $+\boldsymbol{e}_j$, so each contributes $-mv_*$ to the j component of impulse. Arrivals from $\boldsymbol{n}+\boldsymbol{e}_j$ have last step $-\boldsymbol{e}_j$ and contribute $+mv_*$. Adding these two expected rates proves (7). Substitution of (5) proves (8). Independence of the arrival counts over disjoint time intervals is not needed. □

The total encounter rate follows the sum of neighboring populations. The vector force follows their differences. This is why counting all encounters and simply assigning each one a pull toward a remembered source would give a different model. Directional cancellation is essential here.

4.1 Exact direction on the cubic lattice

The force is more structured than its continuum approximation alone suggests. For $\boldsymbol{n} \neq 0$, define

$$\mathcal{J}(\boldsymbol{n}) = \int_0^\infty \frac{K_t(\boldsymbol{n})}{t}\,dt. \tag{9}$$

Theorem 4.2 (Exact central attraction)**.** *For a stationary point source and a nonabsorbing point receiver on the infinite cubic lattice,*

$$\boxed{\boldsymbol{F}(\boldsymbol{n}) = -mv_*qM\,\boldsymbol{n}\,\mathcal{J}(\boldsymbol{n}), \qquad \boldsymbol{n}\neq 0.} \tag{10}$$

The scalar $\mathcal{J}(\boldsymbol{n})$ is finite and strictly positive. Hence the mean force points exactly toward the source at every nonzero lattice separation. Its magnitude need not be the same at different lattice points with the same Euclidean distance from the source.

Proof. The three coordinate walks are independent. Their transition kernels are the differences of independent Poisson processes, giving the product representation

$$K_t(\boldsymbol{n}) = e^{-6t}\prod_{\ell=1}^{3} I_{n_\ell}(2t), \tag{11}$$

where I_k is the modified Bessel function and $I_{-k} = I_k$ for integer k. The representation also follows by expanding the generating function $e^{t(z+z^{-1})}$ in powers of z [2]. The recurrence [3]

$$I_{k-1}(2t) - I_{k+1}(2t) = \frac{k}{t} I_k(2t) \tag{12}$$

therefore implies, including negative or zero n_j,

$$K_t(\boldsymbol{n} + \boldsymbol{e}_j) - K_t(\boldsymbol{n} - \boldsymbol{e}_j) = -\frac{n_j}{t} K_t(\boldsymbol{n}). \tag{13}$$

For $\boldsymbol{n} \neq 0$, the integrand in (9) is $O(t^{|\boldsymbol{n}|_1 - 1})$ near zero and $O(t^{-5/2})$ at infinity. These bounds follow from the small-argument series and fixed-order large-argument asymptotics of the Bessel functions, respectively. The integral converges and is positive. Integrating (13) gives

$$\mathcal{H}(\boldsymbol{n} + \boldsymbol{e}_j) - \mathcal{H}(\boldsymbol{n} - \boldsymbol{e}_j) = -n_j \mathcal{J}(\boldsymbol{n}). \tag{14}$$

Equation (10) now follows from (8). □

This identity is a consequence of standard heat-kernel and Bessel identities, not evidence of a new physical interaction. Exact centrality also holds for a source switched on at time zero: replace the upper integration limit in (9) by γt. It depends on the specified isotropic hopping rule, centered arrival response, point geometry, and absence of boundaries or other modifications to the particle motion.

At $\boldsymbol{n} = 0$, symmetry gives zero mean self-force directly from (7). The integral $\mathcal{J}(0)$ diverges, so (10) must not be evaluated there as a product of zero and infinity. Self-generated returning particles can still produce fluctuations even when the mean self-force is zero.

5 Newtonian behavior and the discrete Poisson equation

Theorem 5.1 (Large-distance force law)**.** *At physical separation $\boldsymbol{x} = h\boldsymbol{n}$ with $r = |\boldsymbol{x}| \gg h$, the stationary mean force has the form*

$$\boldsymbol{F}(\boldsymbol{x}) = -G_{\text{eff}} M m \frac{\boldsymbol{x}}{r^3} [1 + O(h/r)], \qquad \boxed{G_{\text{eff}} = \frac{q v_* h^2}{2\pi}}. \tag{15}$$

The displayed error bound is conservative; no optimal lattice-error order is asserted here.

Proof. The first-difference estimates for the Green function imply the vector asymptotic

$$\left(\mathcal{H}(\boldsymbol{n} + \boldsymbol{e}_j) - \mathcal{H}(\boldsymbol{n} - \boldsymbol{e}_j)\right)_{j=1}^3 = -\frac{\boldsymbol{n}}{2\pi|\boldsymbol{n}|^3} + O(|\boldsymbol{n}|^{-3}). \tag{16}$$

For example, apply the cited first-difference estimate to the two forward differences composing each centered difference, and expand the explicit function $1/|\boldsymbol{n}|$. Choose a coordinate with $|n_j| \geq |\boldsymbol{n}|/\sqrt{3}$ and combine (16) with (14). Then

$$\mathcal{J}(\boldsymbol{n}) = \frac{1}{2\pi|\boldsymbol{n}|^3} + O(|\boldsymbol{n}|^{-4}). \tag{17}$$

Substitution into (10), followed by $\boldsymbol{n}/|\boldsymbol{n}|^3 = h^2\boldsymbol{x}/r^3$, proves the claim. □

The hopping rate cancels from the stationary force because faster hopping reduces the mean residence population by the same factor by which it increases the encounter rate. It still controls the approach to stationarity. The units of qv_*h^2 are length^3 mass^{-1} time^{-2}, as required for a gravitational constant. The parameters must be calibrated so that G_{eff} agrees with the measured Newton constant; the construction does not predict its numerical value.

5.1 An exact potential representation

Define the physical centered difference and physical lattice Laplacian by

$$(D^0_{h,j}f)(\boldsymbol{n}) = \frac{f(\boldsymbol{n}+\boldsymbol{e}_j) - f(\boldsymbol{n}-\boldsymbol{e}_j)}{2h}, \qquad \Delta_h = h^{-2}\Delta_{\mathbb{Z}}. \tag{18}$$

For several fixed sources, write $M(\boldsymbol{n})$ for the total source mass deposited at site $\boldsymbol{n}$ and $\rho_h(\boldsymbol{n}) = M(\boldsymbol{n})/h^3$. Define

$$\Phi_h(\boldsymbol{n}) = -2v_*\gamma h\,\mu_\infty(\boldsymbol{n}). \tag{19}$$

Equations (5) and (7) yield the exact relations

$$\boxed{\Delta_h\Phi_h = 4\pi G_{\text{eff}}\rho_h, \qquad \frac{\boldsymbol{F}}{m} = -\boldsymbol{D}^0_h\Phi_h.} \tag{20}$$

Thus the mean collision rule is a stochastic realization of a particular discrete Poisson force operator. At finite h, a centered difference is not a derivative with respect to a continuously variable body coordinate. Equation (20) alone does not specify a continuous Hamiltonian or a conservative interpolation for off-lattice motion.

5.2 Superposition and reciprocal mean forces

Nonabsorbing receivers do not change the walker field, so source contributions add linearly. If two bodies both emit at rate proportional to mass and use the same v_*, the stationary pair contribution satisfies

$$\boldsymbol{F}_{a\leftarrow b} = -m_a m_b q v_*(\boldsymbol{n}_a - \boldsymbol{n}_b)\,\mathcal{J}(\boldsymbol{n}_a - \boldsymbol{n}_b) = -\boldsymbol{F}_{b\leftarrow a}. \tag{21}$$

It is also exactly central. The frozen-configuration mean pair forces therefore have zero net force and zero net torque. This is stronger than an arbitrary cubic discretization would guarantee. It does not imply equal and opposite individual collision impulses, conservation along stochastic trajectories, or absence of delayed forces when bodies move.

Mass-independent mean acceleration follows from (2). It is built into the model through the response coefficient. A model using a mass-independent impulse per hit would instead need an encounter rate proportional to receiver mass. Finite-size bodies require a specified distribution of emission and response sites; replacing mass by geometric interception area is not automatically equivalent.

6 Many bodies and efficient voxel representations

All particles have the same hopping law and the same effect on a given receiver, regardless of their source. Consequently, different emitters do not require different particle species or separate fields. This permits an exact occupation-count representation. It does not require a physical interaction between the emitted particles.

6.1 An exact stochastic update using population counts

Use the synchronous model of Appendix A, with tick duration τ. For this section, let the body sites be fixed or specified externally at each tick. A body remains at its assigned site during that tick's hopping and collision stage. Write

$$M_k(\boldsymbol{n}) = \sum_{a:\, \boldsymbol{n}_a(k)=\boldsymbol{n}} m_a \tag{22}$$

for source mass at a site, and let $N_k(\boldsymbol{n})$ be the total particle count before the hops. Put $\mathcal{S} = \{\pm \boldsymbol{e}_1, \pm \boldsymbol{e}_2, \pm \boldsymbol{e}_3\}$. At every site, draw outgoing counts jointly as

$$(L_{k,\boldsymbol{s}}(\boldsymbol{n}))_{\boldsymbol{s}\in\mathcal{S}} \mid N_k \;\sim\; \text{Multinomial}\left(N_k(\boldsymbol{n}); \tfrac{1}{6}, \tfrac{1}{6}, \tfrac{1}{6}, \tfrac{1}{6}, \tfrac{1}{6}, \tfrac{1}{6}\right). \tag{23}$$

These draws are conditionally independent at distinct departure sites. The count arriving at $\boldsymbol{n}$ with last step $\boldsymbol{s}$ is

$$A_{k,\boldsymbol{s}}(\boldsymbol{n}) = L_{k,\boldsymbol{s}}(\boldsymbol{n} - \boldsymbol{s}). \tag{24}$$

After recording arrivals, draw new emission counts independently of the hopping draws and independently across sites,

$$B_k(\boldsymbol{n}) \sim \text{Poisson}(q\tau M_k(\boldsymbol{n})). \tag{25}$$

Then update the population and the impulse on each body a at its current site:

$$N_{k+1}(\boldsymbol{n}) = \sum_{\boldsymbol{s}\in\mathcal{S}} A_{k,\boldsymbol{s}}(\boldsymbol{n}) + B_k(\boldsymbol{n}), \tag{26}$$

$$\Delta \boldsymbol{P}_{a,k} = -m_a v_* \sum_{\boldsymbol{s}\in\mathcal{S}} \boldsymbol{s}\, A_{k,\boldsymbol{s}}(\boldsymbol{n}_a(k)). \tag{27}$$

If several bodies occupy one site, each receives the prescribed impulse per arrival; this follows the paper's nonabsorbing point-receiver rule. Newborn particles do not contribute to that tick's arrivals.

Proposition 6.1 (Exact aggregation of indistinguishable walkers)**.** *For the synchronous collision model, equations* (23)–(27) *have the same joint law of voxel occupations and tick impulses as individually tracked particles, after discarding particle labels. This holds for any finite collection of sources and receivers and any finite number of ticks, with matching initial count distributions and the same boundary convention.*

Proof. Conditional on the current count at a site, every labeled walker independently chooses one of the six steps. Counting those categorical choices gives exactly the multinomial law in (23). Choices at different sites are independent. Arrivals are obtained by moving the corresponding counts to their destinations, and the collision impulse is their signed sum; it does not use a particle's identity or previous trajectory. The sum of independent Poisson emissions by co-located bodies is Poisson with parameter $q\tau M_k(\boldsymbol{n})$. These statements identify the same conditional transition law for the count-and-impulse variables in both descriptions. Induction over ticks gives equality of their joint laws, including fluctuations and temporal correlations. □

The proof relies on the memoryless, source-independent transition and response rules. In particular, particles returning to their own emitter are included, as in the baseline model. Excluding such returns by emitter identity, assigning different properties to different source particles, or retaining directional persistence would require additional state. The equivalence between voxel counts and labeled lattice walkers is an established principle in stochastic diffusion [10]; here the directed arrivals also retain the information needed for the proposed collision impulses.

The aggregation remains exact for a specified coupled tick model if bodies are advanced after the collision stage by a rule depending only on retained body state and aggregate impulses, and the next deposition uses those updated sites. It preserves that chosen stochastic model, but does not supply the missing body-motion law or establish its physical correctness. For continuous-time walkers, a count process with directed jump rates γN is also exact. Replacing an arbitrary continuous-time interval by a single multinomial draw over final destinations would generally lose intermediate encounters and their impulses; our tick theorem makes no such replacement.

6.2 Computational cost and the meaning of merging

Store one integer population per voxel, a next-step buffer, and temporary directional transfers or equivalent arrival accumulators. Record collision impulses before discarding the incoming directions. The next random step has no memory of the previous direction, so a persistent trajectory record is unnecessary.

For V processed voxels and B bodies, this uses $O(V+B)$ stored numbers, compared with $O(N_{\text{particles}}+B)$ particle records. Each tick uses one six-category draw per occupied departure voxel, at most six transfers per such voxel, and deposition and response work proportional to B. With suitable population samplers and fixed-width arithmetic, this gives approximately $O(V+B)$ work per tick. It is an operation-count description, not a benchmark or a bound on arbitrary-precision bit complexity. Naively implementing each multinomial draw by looping over all particles would forfeit the saving. Nor is voxel processing automatically faster in an enormous, mostly empty domain. Counts can be stored sparsely, but the active domain can still grow over time.

Aggregation means preserving multiplicity in a counter. It is different from replacing N independent walkers by one walker of weight N that follows a single shared path. For a specified outgoing direction with probability $p = 1/6$, the independent count has variance $Np(1-p)$; the weighted walker's outgoing weight has variance $N^2p(1-p)$. The means agree, but the latter creates artificial collective fluctuations. Exact stochastic aggregation must retain the multinomial split or an equivalent sampling procedure.

6.3 Cancellation of impulses is not annihilation of particles

Suppose a receiver gets 100 arrivals from each of two opposite directions during a tick. Those 200 assigned impulses sum to zero, so the body update can use a single net value. However, the voxel contains 200 surviving walkers, and their subsequent departures influence other sites and later collisions. Deleting them because their present impulses cancel changes the next transition law.

An empty voxel and a voxel containing those 200 walkers can therefore have the same net impulse during one tick but different future behavior. This is a direct reason that storing only the current three-component impulse cannot reproduce the full particle process. All baseline walkers contribute positive occupation and have identical rules; arrivals from opposite directions are not distinct positive and negative species that annihilate. A physical annihilation rule would add a new sink or reaction term and require a fresh force-law analysis.

6.4 Deterministic fields and direct evolution of acceleration

For externally prescribed body sites, let $u_k(\boldsymbol{n}) = \mathbb{E}N_k(\boldsymbol{n})$ and let P denote six-neighbor averaging. Taking expectations in (26) gives the exact mean update

$$u_{k+1} = Pu_k + q\tau M_k, \qquad (Pu)(\boldsymbol{n}) = \frac{1}{6}\sum_{\boldsymbol{s}\in\mathcal{S}} u(\boldsymbol{n}-\boldsymbol{s}). \tag{28}$$

Only one shared scalar field is needed for all emitters. Define the dimensionless centered difference

$$(\mathcal{D}_j u)(\boldsymbol{n}) = u(\boldsymbol{n}+\boldsymbol{e}_j) - u(\boldsymbol{n}-\boldsymbol{e}_j), \qquad a_{j,k}(\boldsymbol{n}) = \frac{v_*}{6\tau}\mathcal{D}_j u_k(\boldsymbol{n}). \tag{29}$$

Here $a_{j,k}$ is the mean acceleration inferred from the next hopping stage at a fixed query site. On the infinite lattice, or a periodic grid with consistent shifts, $P\mathcal{D}_j = \mathcal{D}_j P$. Applying $\mathcal{D}_j$ to (28) proves the closed recurrence

$$\boxed{a_{j,k+1} = Pa_{j,k} + \frac{qv_*}{6}\mathcal{D}_j M_k, \qquad j = 1,2,3.} \tag{30}$$

With consistent initial conditions, this evolves the deterministic acceleration directly using three signed numbers per voxel. Opposing source contributions cancel algebraically. A spatially uniform part of u_k need not be stored because its centered differences vanish. Boundary conditions that break translation invariance require their own compatible treatment; the commutation argument cannot simply be assumed there.

Equations (28) and (30) describe identical mean-force calculations for prescribed sources, subject to numerical precision. They do not retain the particle fluctuations. For bodies moving in response to the random field, evaluating a deterministic field along a deterministic trajectory is not generally the expectation of the stochastic trajectory: the body positions and field are correlated. Thus the direct-field scheme is an economical deterministic approximation for that coupled problem, not an exact reduction of its full law.

6.5 Finite numbers of variables and finite numbers of bits

A fixed number of variables per voxel does not make their exact state space finite. A counter able to represent every occupation from zero through $N_{\max}$ needs at least $\lceil \log_2(N_{\max}+1)\rceil$ bits. The baseline Poisson emission and occupation processes admit arbitrarily large counts, even when the stationary mean at a particular site is finite. Hence no fixed-width counter represents the unrestricted process exactly for every possible realization.

Practical integer counts are faithful while the chosen range is respected; an implementation should detect overflow rather than silently wrap or clip. Floating-point mean fields instead introduce finite precision. A hard occupancy cap, exclusion rule, saturation response, or particle deletion defines different dynamics. A bounded-state cellular automaton may still be an interesting microscopic proposal, but its mean force, fluctuations, and departure from source superposition would have to be derived separately. None of these changes is justified merely by calling it compression.

The count representation is therefore a natural next implementation of the emitted-particle model. A deterministic field implementation provides a useful reference for its mean behavior. Developing an exactly finite-state microscopic theory is a further modeling task, not a requirement for eliminating individual particle records from a simulation.

Representation	Quantity or law preserved
Counts with multinomial transfers	Full synchronous occupation and collision-impulse law, with exact counters and the same update rules.
One weighted walker per group	Expected transport; shared trajectories alter fluctuations and correlations.
Scalar mean field or three acceleration fields	Deterministic mean force for prescribed sources; collision noise is absent.
Annihilation or bounded occupancy	A modified microscopic process; the gravitational limit must be checked again.

Table 1: Computational aggregation and changes to the microscopic model have different mathematical consequences.

7 Time dependence and particle fluctuations

7.1 The diffusion delay

For a point source switched on at time zero, the continuum density approximation is

$$c(r,t) = \frac{qM}{4\pi D r}\,\mathrm{erfc}\left(\frac{r}{2\sqrt{Dt}}\right), \qquad c \simeq \mu/h^3. \tag{31}$$

To derive it, integrate the three-dimensional heat kernel $(4\pi Ds)^{-3/2}\exp[-r^2/(4Ds)]$ over source ages $0 < s < t$ and substitute $u = r/(2\sqrt{Ds})$. Expanding (7) in physical coordinates gives $\boldsymbol{F} \simeq 2mv_*\gamma h^4 \nabla c$. Consequently,

$$\boldsymbol{F}(r,t) \simeq -G_{\mathrm{eff}} M m \frac{\hat{\boldsymbol{r}}}{r^2}\left[\mathrm{erfc}(\xi) + \frac{2\xi}{\sqrt{\pi}} e^{-\xi^2}\right], \quad \xi = \frac{r}{2\sqrt{Dt}}. \tag{32}$$

The familiar inverse-square value is approached when $t \gg r^2/D$. A quasi-static treatment of a slowly changing source distribution requires this relaxation time to be short compared with the timescale of the source motion; it is not a theorem about arbitrary moving bodies.

The continuous-time random walk permits arbitrarily many hops in a finite interval, with small but nonzero probability, and therefore has no strict finite signal speed. The synchronous alternative in Appendix A has a maximum reach of one lattice edge per tick, but its bulk spreading remains diffusive. Neither fact establishes relativistic gravitational propagation.

7.2 A precise description of collision noise

The mean force is not the full stochastic model. For a fixed receiver, let $A_j^-(T)$ count arrivals from $\boldsymbol{n} - \boldsymbol{e}_j$ and $A_j^+(T)$ arrivals from $\boldsymbol{n} + \boldsymbol{e}_j$. Then

$$I_j(T) = mv_*[A_j^+(T) - A_j^-(T)]. \tag{33}$$

Given the entire particle configuration, the conditional arrival intensities are $\gamma N(\boldsymbol{n} \pm \boldsymbol{e}_j, t)$. The compensated impulse

$$\mathcal{M}_j(T) = I_j(T) - mv_*\gamma \int_0^T [N(\boldsymbol{n}+\boldsymbol{e}_j,t) - N(\boldsymbol{n}-\boldsymbol{e}_j,t)]\,dt \tag{34}$$

is a martingale. Its predictable quadratic variation is

$$\langle \mathcal{M}_j \rangle_T = (mv_*)^2 \gamma \int_0^T [N(\boldsymbol{n}+\boldsymbol{e}_j, t) + N(\boldsymbol{n}-\boldsymbol{e}_j, t)]\, dt. \tag{35}$$

This follows by adding squared jump sizes times their conditional rates. In stationarity, its expectation divided by T is

$$\frac{\mathbb{E}\langle \mathcal{M}_j \rangle_T}{T} = (mv_*)^2 \gamma [\mu_\infty(\boldsymbol{n}+\boldsymbol{e}_j) + \mu_\infty(\boldsymbol{n}-\boldsymbol{e}_j)]. \tag{36}$$

Far from the source this local noise rate scales as $1/r$, whereas the mean force scales as $1/r^2$. This is not a formula for the full variance of $I_j(T)$: occupation fluctuations and repeated visits correlate the arrival process and its random compensator. A white-noise or independent-Poisson approximation would require additional justification.

There is a controlled computational way to reduce fluctuations. Combine K independent copies of the emission process and divide every kick by K. Equivalently, replace q by Kq and v_* by v_*/K. The mean force and G_{eff} are unchanged. For fixed receivers over a finite observation interval, independent replication reduces impulse variance by $1/K$ whenever that variance is finite. The number of simulated particles increases by the same factor. This is a sampling refinement, not a microscopic explanation for a noise-free physical gravitational field.

8 Numerical verification on the infinite cubic lattice

We evaluate the exact stationary formulas by deterministic quadrature of (11) and (9). These calculations have no finite-box boundary and do not simulate moving bodies or individual particle collisions. Their purpose is to check constants, force direction, and the magnitude of lattice corrections.

Exponentially scaled Bessel functions evaluate $e^{-2t} I_k(2t)$ without overflowing. For arguments exceeding 2×10^6, we use the large-argument expansion through the term of order eight [4] to avoid numerical failure in the special-function library. With $R = \max(1, |\boldsymbol{n}|)$, the substitution $t = R^2/(4u^2)$ gives integrable, smooth long-time endpoints. We integrate in four intervals, $[0, 1/4]$, $[1/4, 1]$, $[1, 4]$, and $[4, \infty)$, using adaptive quadrature. The accompanying Python script records the tolerances and the library versions.

First, we compute the force in two algebraically equivalent but numerically independent ways: by subtracting separately integrated Green values in (8), and by evaluating $-\boldsymbol{n}\mathcal{J}(\boldsymbol{n})$. The tested vectors are $(1, 0, 0)$, $(2, 1, 0)$, $(3, 2, 1)$, $(8, 3, 2)$, and $(16, 0, 0)$. We also check the source normalization $6[\mathcal{H}(\boldsymbol{e}_1) - \mathcal{H}(0)] = -1$. The executable verification asserts relative vector agreement below 10^{-7} and source residual below 10^{-8}; these are numerical consistency checks, not replacements for the proofs above.

Second, define the force ratio

$$A(\boldsymbol{n}) = \frac{|\boldsymbol{F}(\boldsymbol{n})|}{G_{\text{eff}} Mm/(h^2 |\boldsymbol{n}|^2)} = 2\pi |\boldsymbol{n}|^3 \mathcal{J}(\boldsymbol{n}). \tag{37}$$

We compare points $(5k, 0, 0)$ and $(3k, 4k, 0)$, which have the same Euclidean distance, for $k = 1, 2, 4, 8$. Unity is the Newtonian limit. "Directional spread" is the absolute difference of the two ratios, not an uncertainty estimate.

r/h	Axis ratio	3–4–5 ratio	Directional spread
5	1.08764596	0.99414469	0.09350127
10	1.01829365	0.99759257	0.02070108
20	1.00442043	0.99935003	0.00507040
40	1.00109654	0.99983468	0.00126186

Table 2: Computed stationary force ratios at equal separations. Values describe the specified mathematical model and are not measurements of physical gravity.

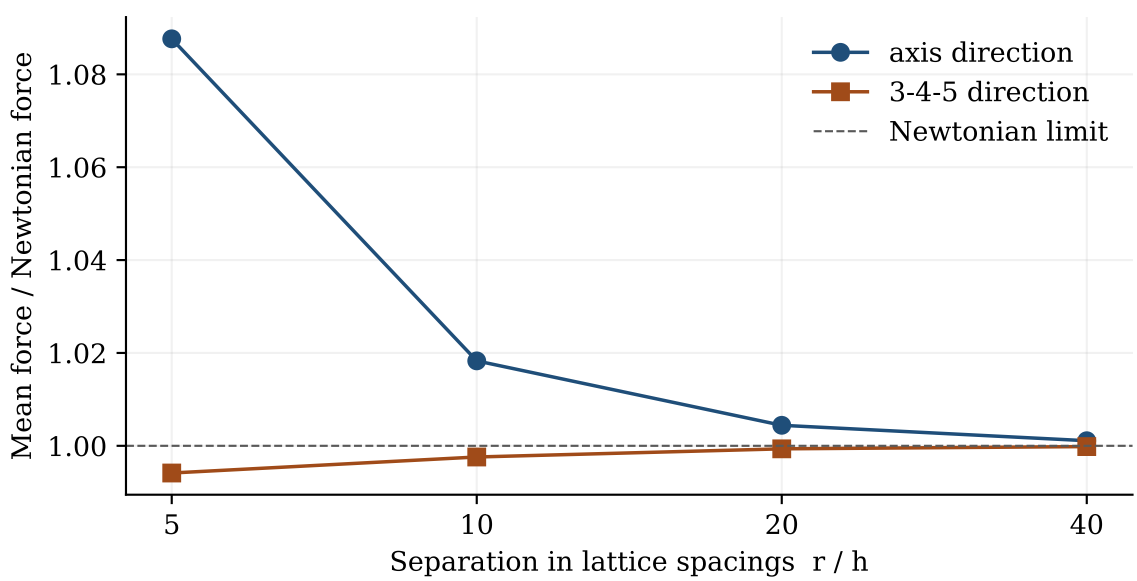

Figure 1: Approach to the inverse-square magnitude along two lattice directions. Exact centrality of the force does not imply exact rotational invariance of its strength.

At five lattice spacings the axis force is about 8.76% above the Newtonian value, while the 3–4–5 direction is about 0.586% below it. At forty spacings the corresponding deviations are about 0.110% and 0.0165%. The sample establishes neither a uniform error bound over all directions nor orbital accuracy. It displays a concrete lattice effect that a physical interpretation would have to confront or make sufficiently small.

9 Comparison with existing models

The stationary population and its $1/r$ asymptotic are standard Green-function results. The Gaussian-to-Poisson connection is therefore not new. Monte Carlo methods can calculate gravitational potentials using random paths, including paths started at a query point and stopped at a boundary [5]. The present formulation instead starts walkers at emitting masses and assigns signed impulses to receiving bodies. Its mean reduces exactly to the discrete Poisson representation (20).

The mechanism differs from Le Sage's historical bombardment proposal. There, a roughly isotropic external particle background pushes bodies together because each body partially shields the other. In the present model the bodies supply the particles and attraction is imposed by the sign of the encounter response. Feynman's discussion of bombardment gravity identifies orbital drag as a failure of the simple shielding picture [7]. It does not by itself analyze the different stochastic rules used here.

Quantum-gravitational exchange is another distinct construction. Low-energy quantum general relativity has an effective-field-theory description involving gravitons [8]. Virtual exchange in that framework is not a classical random walk of emitted objects that register backward kicks on arrival. We therefore do not identify the proposed walkers with gravitons.

The exact centrality result above follows from a standard Bessel recurrence applied to the specified collision rule. We make no claim that this mathematical identity, the general emission idea, or this precise interpretation has historical priority. Establishing such priority would require a dedicated literature review beyond the foundational comparisons used here.

10 Physical requirements and limitations

10.1 Momentum and energy at individual encounters

The baseline process does not conserve the momentum of particles and bodies as a closed mechanical system. If a conventional particle arrives moving in $+\boldsymbol{e}_j$ and is absorbed, its ordinary momentum transfer is positive in that direction. Rule (2) prescribes the opposite. Moreover, our walker leaves its encounter with unchanged stochastic rules while the receiver has acquired an impulse. A compensating change in a particle, lattice, or other degree of freedom has not been specified.

Even between encounters, a conventional particle changing direction during a random walk would exchange momentum with something. The lattice in the present formulation supplies locations and transition rules, but has no dynamical variables capable of storing recoil or energy. Adding those variables could define a different model; it would require rechecking the mean force rather than assuming the current derivation survives.

If the receiver were allowed to move, a kick $-mv_*\boldsymbol{s}$ would change its kinetic energy by

$$\Delta E_{\mathrm{kin}} = -mv_*\boldsymbol{v}\cdot\boldsymbol{s} + \frac{1}{2}mv_*^2. \tag{38}$$

The positive quadratic term illustrates the need to analyze stochastic heating. The model gives no compensating microscopic energy balance. If emitted walkers are instead physical particles with positive energy, continuing emission also requires an energy source and associated source bookkeeping. Exact reciprocal forces in the stationary mean do not resolve either issue.

10.2 Moving bodies and the preferred lattice

A cubic lattice selects spatial axes and, with a clock or hopping rates, a preferred rest frame. The force magnitude retains cubic directional dependence at finite separation, as Table 2 shows. The model does not supply Lorentz symmetry, gravitational time dilation, light deflection, or gravitational waves. Studies of hypothetical fundamental lattices discuss possible symmetry-breaking signatures [9]; they do not establish that physical space is such a lattice.

For moving sources, walkers sample past source positions. Self-emitted particles may return after their source has moved, and the stationary symmetry argument for zero self-force then no longer applies. A moving body also needs a rule for lattice occupancy, subcell position, or integer displacement accumulation. No stable-orbit result is claimed here. A continuum limit at fixed measured gravity additionally requires scaling $qv_* \propto h^{-2}$ as $h \to 0$; holding every microscopic parameter fixed would instead drive G_{eff} to zero.

10.3 Boundaries and particle removal

The theorems assume unlimited particle lifetime and an infinite lattice. In a closed finite box, persistent emission makes the mean total population grow without bound. Some population differences may settle while the uniform component grows, but that does not give a stationary particle field or stationary collision noise. An escape boundary makes a finite computation possible and changes the Green function.

If particles disappear independently at rate $\lambda > 0$, the continuum steady equation becomes $D\Delta c - \lambda c = -qM\delta_0$. Its point-source solution and the resulting force magnitude are proportional to

$$c(r) = \frac{qM}{4\pi D r}e^{-r/\ell}, \qquad |\boldsymbol{F}(r)| \simeq G_{\mathrm{eff}}Mm\, e^{-r/\ell}\left(\frac{1}{r^2} + \frac{1}{\ell r}\right), \quad \ell = \sqrt{D/\lambda}. \tag{39}$$

Thus deleting walkers to save computation changes the long-range law unless its effect is controlled. Absorbing or scattering receivers likewise change the population problem and are outside the nonabsorbing theorem.

11 Conclusion

Emitted random walkers on a cubic lattice can produce an attractive mean force when a collision gives the receiver a kick opposite the walker's last step. For the explicitly defined nonabsorbing model, the force is exactly central for a fixed point source and approaches the Newtonian inverse-square magnitude at large separation. The mean is governed by a discrete Poisson equation, with $G_{\mathrm{eff}} = qv_*h^2/(2\pi)$.

For many bodies, emitter identities and individual particle records are unnecessary under the specified rules. Population counts with multinomial transfers preserve the synchronous stochastic process, including its collision fluctuations. A scalar mean field or three directly evolved acceleration fields provide deterministic alternatives, while particle annihilation and hard occupancy bounds change the model. The distinction between a fixed number of voxel variables and a fixed number of bits is essential when proposing a finite-state universe simulation.

The construction clarifies what the proposal supplies: local events and directional cancellation realize a known gravitational mean-field operator. It also clarifies what is assumed: the attractive collision sign, response proportional to receiver mass, emission proportional to source mass, and unchanged walker dynamics. A physical theory would have to supply conserved microscopic dynamics, control fluctuations, and reproduce gravitational observations beyond this stationary Newtonian regime. Those are concrete next problems, not consequences already proved by the present model.

A A synchronous cubic lattice implementation

The idea can be implemented with a global tick of duration τ. At each tick, every existing particle takes exactly one of the six allowed steps with probability $1/6$. Every registered arrival at a body of mass m gives the impulse (2). After the hops, a source of mass M emits a Poisson number of particles with mean $qM\tau$. New particles first hop on the next tick. The body sites are held fixed for a direct comparison with the theorems.

If P denotes neighbor averaging, the mean population update is

$$\mu_{k+1} = P\mu_k + qM\tau\delta_0, \qquad P = I + \frac{1}{6}\Delta_{\mathbb{Z}}. \tag{40}$$

Since $\sum_{k\geq 0} P^k\delta_0 = 6\mathcal{H}$, the stationary local occupation is $\mu_\infty = 6qM\tau\mathcal{H}$. The expected force is the mean impulse per tick divided by τ:

$$F_j = \frac{mv_*}{6\tau}[\mu_\infty(\boldsymbol{n}+\boldsymbol{e}_j) - \mu_\infty(\boldsymbol{n}-\boldsymbol{e}_j)] = mv_*qM[\mathcal{H}(\boldsymbol{n}+\boldsymbol{e}_j) - \mathcal{H}(\boldsymbol{n}-\boldsymbol{e}_j)]. \tag{41}$$

Thus it has precisely the same stationary force as (8). The associated diffusion coefficient is $D = h^2/(6\tau)$, matching the continuous-time choice $\gamma = 1/(6\tau)$. Its reachable set after k ticks lies inside $|\boldsymbol{n}|_1 \leq k$ for a particle born at the origin; the bulk distribution spreads over order $\sqrt{k}$ lattice spacings.

Section 6 gives the exact count-based update for many bodies and proves its equivalence to tracking individual particles. A direct implementation follows this order:

1. Read the current body sites, masses, and voxel populations. Clear the next-population and impulse buffers.
2. At each occupied voxel, draw its six outgoing counts jointly according to (23).
3. Transfer each directed count to its neighboring destination and accumulate the signed collision response there using (27).
4. Add independent Poisson emissions with mean $q\tau M_k(\boldsymbol{n})$ to the destination population buffer. These new particles wait until the next tick to hop.
5. Record the impulses and swap the population buffers. For a coupled moving-body extension, apply the explicitly chosen body-motion rule after the collision stage and use its new sites for the next tick.

The fixed-body calculation ends with recorded impulses; it does not update body positions. Replacing the multinomial counts by their means produces a deterministic occupation update and removes the packet fluctuations.

This is a stochastic lattice process with unbounded occupation counts. It is not, as written, a deterministic finite-state cellular automaton. Additional state and encoding choices would be needed to impose that restriction.

B Reproducibility

The accompanying source package contains this manuscript, `verify_model.py`, its generated data and figure, and a README with build instructions. Run the Python script with NumPy, SciPy, and Matplotlib installed, then run `pdflatex` twice on the manuscript. The calculations evaluate the infinite-lattice mean force. The included synchronous implementation is specified mathematically; a particle Monte Carlo experiment, moving-body simulation, and comparison with astronomical observations have not been performed for this paper.

An accompanying interactive 3D visualization of the proposed model is available at `https://zoan.space/viz/gravity/`.

References

[1] G. F. Lawler and V. Limic. *Random Walk: A Modern Introduction*. Cambridge University Press, 2010. Chapters 2 and 4. https://www.math.uchicago.edu/~lawler/srwbook.pdf.

[2] NIST Digital Library of Mathematical Functions. Section 10.35, Generating Function and Associated Series. https://dlmf.nist.gov/10.35.

[3] NIST Digital Library of Mathematical Functions. Section 10.29, Recurrence Relations and Derivatives. https://dlmf.nist.gov/10.29.

[4] NIST Digital Library of Mathematical Functions. Section 10.40, Asymptotic Expansions for Large Argument. https://dlmf.nist.gov/10.40.

[5] F. Donzelli, A. Bihlo, M. Kischinhevsky, and C. G. Farquharson. Massively parallel stochastic solution of the geophysical gravity problem. 2017. arXiv:1709.07469. https://arxiv.org/abs/1709.07469.

[6] J. P. Ramsey, T. Haugbølle, and Å. Nordlund. A simple and efficient solver for self-gravity in the DISPATCH astrophysical simulation framework. 2018. arXiv:1806.10098. https://arxiv.org/abs/1806.10098.

[7] R. P. Feynman, R. B. Leighton, and M. Sands. *The Feynman Lectures on Physics*, Volume I, Chapter 7, The Theory of Gravitation. Caltech online edition. https://www.feynmanlectures.caltech.edu/I_07.html.

[8] J. F. Donoghue. Quantum General Relativity and Effective Field Theory. 2022, revised 2023. arXiv:2211.09902. https://arxiv.org/abs/2211.09902.

[9] S. R. Beane, Z. Davoudi, and M. J. Savage. Constraints on the Universe as a Numerical Simulation. 2012. arXiv:1210.1847. https://arxiv.org/abs/1210.1847.

[10] S. A. Isaacson. Relationship between the reaction–diffusion master equation and particle tracking models. *Journal of Physics A: Mathematical and Theoretical* 41 (2008), 065003. https://doi.org/10.1088/1751-8113/41/6/065003.